

Geometric Methods for Analysis of Electrocardiogram Anomalies Associated with Critical Events in Children with Congenital Heart Disease.

Freddy Angarita

School of Electrical and Computer Engineering

Rice University

Houston, Texas

Email: faa3@rice.edu

Abstract—Junctional ectopic tachycardia (JET) is a type of arrhythmia that usually emerges as an early postoperative symptom in patients that go under open heart surgery to repair a congenital heart disease (CHD) [3]. Current JET detection methods require physicians to look for abnormalities in ECG recordings which can be cumbersome and prone to error. The purpose of this work was to preprocess ECG recordings into probability distributions with the Hilbert transform so that geometric methods can be used for the detection of JET heartbeats. Two geometric distances, Euclidean and Wasserstein, were computed to analyze the distance between a healthy and a JET heartbeat. This report shows that both distances can be used to identify JET heartbeats, and as a result, a new algorithmic framework can be fused with geometric distances and machine learning to detect arrhythmic anomalies during prolonged periods before critical events occur.

1. Introduction

Congenital Heart Disease (CHD) refers to heart defects or abnormalities present at birth. CHD has become a major global health problem as it affects approximately 8 out of every 1,000 live births [12]. Post operative junctional ectopic tachycardia (JET) is a type of cardiac arrhythmia that occurs immediately after an open heart surgical repair of CHD. Risk factors for JET include younger age, lower weight, longer cardiopulmonary bypass (CBP), and hyperthermia, among others. A study shows that JET is more likely to occur after intravenous administration of inotropic agents due to low cardiac output, which produces high adrenergic stress [9].

JET can occur in 15.3% of children and young adults undergoing open heart surgery leading to longer ICU stays and higher mortality rates [9]. JET is commonly defined as a supraventricular arrhythmia, or rapid heartbeat, with no preceding P wave at a rate that exceeds the normal junctional escape rate at a given age.

In an electrocardiogram (ECG), JET is distinguished by the disappearance of the P wave or the appearance of the retrograde P wave [13]. Although the QRS complex of a JET heartbeat can be very fast and narrow, it is still fundamentally very similar to that of a normal sinus heartbeat. This scenario makes the detection of JET occurrence

much more cumbersome for physicians. Current diagnosis methods are based on clinical notes, nursing observations, and the assessment of ECG recordings. Additionally, it has been shown that early treatment of postoperative JET benefits the arrhythmia control and significantly reduces the pediatric cardiac ICU stay [4]. Therefore, there is a need for an automated, data-driven, algorithmic framework that can constantly monitor patients and alert cardiologists of a potential JET occurrence.

The current literature shows that current ECG-based JET detection methods can be grouped in how they do feature selection. Some methods collect features based on width, peak amplitude, or correlation values [7]. However, these feature are too simple and may not extract enough information to accurately identify JET heartbeats. Other methods based on deep learning offer high accuracy but their feature selection process is not interpretable for cardiologists [8]. Moreover, deep learning models require extensive amount of data and high computational power which makes them not suitable for ambulatory care.

The main goal of this project is to develop a personalized monitoring system that can summarize waveform ECG data from extended periods of time to assist in the early detection of heartbeat anomalies. A geometric-based metric is proposed to process heartbeat information to differentiate between a normal sinus heartbeat and patient-specific abnormalities. In this report, I will discuss the results from the first stage which consists of preprocessing ECG recordings into probability distributions using signal processing techniques, and data exploration, where I discuss how geometric based metrics can detect variations in ECG recordings that show the presence of JET arrhythmia.

2. Methods

2.1. Data Collection

The data utilized in this stage comes from 21 patients who were admitted into intensive care units at Texas Children's Hospital. They were monitored using standard monitoring equipment with data being captured by the Sickbay platform. The Sickbay platform consists of software-based

algorithms that convert physiological data from medical devices into real-time data for clinical and research purposes. The data files include ECG signal, as well as pressure measurements, chest impedance, and heart rate. The ECG data used in this report consists of approximately 16 hours of recordings consisting of both normal normal sinus heartbeats and JET heartbeats per patient with the JET heartbeats labeled by physicians from the Texas Children's Hospital. After processing the ECG signals, approximately 90,000 heartbeats were computed and transformed into numerical arrays formats of 101 dimensions. This method of data preprocessing will be explained further in the following subsections.

2.2. Short Time Fourier Transform

The Short-Time Fourier Transform (STFT) consists of breaking a longer signal into small time windows, and then computing the Fourier Transform of each segment. The STFT is a powerful technique to analyze non stationary signals whose frequency components change over time [6]. ECG signals exhibit non stationary characteristics due to changes in heart rate, arrhythmia, or other cardiac events. The output of the STFT is 2D plot of time vs frequency indicating the magnitude of a given frequency at a certain time. However, one of the drawbacks of the STFT is the resolution, as we decrease the time window, we obtain high time resolution but low frequency resolution. Conversely, as we increase the time window, we get better frequency resolution but low time resolution.

2.3. Hilbert Transform

The Hilbert transform is a mathematical operation that results in the convolution of a signal $x(k)$ with the function $1/\pi k$. The Hilbert transform can be used to compute the analytical signal of a sampled function $z(k)$. The analytical signal will be a complex function that contains the information of the real signal's amplitude as well as the phase.

$$z(k) = x(k) + jHx(k) \quad (1)$$

Once the Hilbert transform is computed, the amplitude and the phase of the analytical signal can be computed as,

$$A(k) = |z(k)| ; \phi(k) = \arg(z(k)) \quad (2)$$

Since $A(k)$ and $\phi(k)$ are steady signals, it is possible to perform linear interpolation to estimate the value of the real signal at any point k [1].

2.4. Multidimensional Scaling

Multidimensional Scaling (MDS) is a powerful tool to measure similarity judgements. MDS is a statistical tool that receives as input the similarity estimate of a group of items, and it returns a map that illustrates the spatial relationships among these items [5]. Similar items are kept close to each

other, while dissimilar items are placed further apart. With this technique, we can observe underlying dimensions of the data, which can result in the detection of clusters for classification purposes and data analysis. MDS can be useful to reduce the dimensionality of the data while preserving important relationships among data points.

2.5. Optimal Transport Metric and Barycenters

The detection of JET arrhythmia is essentially a geometric process as it involves the shape analysis of the QRS-complex and the P-wave. This is the motivation behind the study of geometric based models for the automatic detection of cardiac abnormalities.

Optimal transport (OT) is based on the distances between two probabilities distributions, also known as *Wasserstein distance*. One way to understand Optimal Transport is as an Assignment problem where we have a source and a target distribution that live in two different spaces Ω_1 and Ω_2 . Assume also that we are given a Cost matrix C_{ij} indicating the cost of moving one unit of mass from location $i \in \Omega_1$ to location $j \in \Omega_2$. We are tasked to come up with the most efficient plan to move the entire source distribution to the target distribution given the Cost matrix [11]. If the source and target distributions are two discrete probability distributions, then the most efficient plan will have a minimized cost and that cost is known as the Wasserstein distance between those two distributions.

In this report, we consider two discrete one-dimensional probability distributions P and Q with n bins each, and a cost matrix defined as,

$$C_{ij} = ||i - j||^2 \quad (3)$$

The transport plan in the discrete case will be a matrix $T \in R^{n \times n}$. Consequently, we define the total cost as,

$$Total\ Cost = \sum_{i=1}^n \sum_{j=1}^n T_{ij} C_{ij} \quad (4)$$

The optimal transport plan is thus defined by the following optimization problem,

$$\begin{aligned} \min_T \quad & \sum_{i=1}^n \sum_{j=1}^n T_{ij} C_{ij} \\ \text{s.t.} \quad & \sum_{j=1}^n T_{ij} = P_i \quad \forall i \in 1, \dots, n \\ & \sum_{i=1}^n T_{ij} = Q_j \quad \forall j \in 1, \dots, n \\ & T_{ij} \geq 0 \end{aligned} \quad (5)$$

In the optimization problem, the constraints ensure that the marginal probabilities of P and Q match those of the transport plan T . If we define T^* as the solution to the

optimization problem, then the p-Wasserstein distance is defined as,

$$W_p(P, Q) = \left(\sum_{i=1}^n \sum_{j=1}^n T_{ij}^* C_{ij} \right)^{1/p} \quad (6)$$

In the case, where $p = 1$, then there exists a closed form solution for the Wasserstein distance [10],

$$W_1(P, Q) = \sum_{k=1}^n |F_P(k) - F_Q(k)| \quad (7)$$

From the idea of Euclidean mean or Euclidean barycenter, we can extend this knowledge to Optimal Transport and compute a Wasserstein mean or barycenter. In practice, the barycenter can be computed by solving the regularized optimization problem,

$$\min_{\mu} \sum_i W_2^2(\mu, \mu_i) + \gamma E(\mu) \quad (8)$$

With E defined as a penalty function. In the literature, there has been studies proving the convergence and uniqueness of this optimization problem [2].

2.6. Data Processing

Heartbeat arrays were derived from the ECG signals through a series of steps. Initially, the Short-Time Fourier Transform (STFT) was applied to the ECG signal, establishing a time-based frequency representation. Subsequently, a bandpass filter was employed to remove frequency components not pertinent to the individual patient's heartbeat range. The resultant filtered signal underwent an inverse STFT to prepare for the computation of the Hilbert transform.

The analytical signal obtained through the Hilbert transform provided the phase of the signal at all sampled time points. These phase values were then unwrapped, considering each full 2π cycle as indicative of a complete heartbeat. Subsequently, the analytical signal of the ECG recording was employed to interpolate each heartbeat, generating 100 time points per cycle/heartbeat.

2.7. Data Analysis

To discern between sinus and JET heartbeats based on geometric metrics, both Euclidean and Wasserstein distances were calculated. The computation involved determining the Euclidean and Wasserstein barycenters of the complete set of heartbeats, aiming to identify similarities among heartbeats across all patients.

Furthermore, a per-patient analysis was conducted, organizing their heartbeats chronologically to observe potential temporal variations in behavior. Additionally, pairwise Euclidean and Wasserstein distances between heartbeats per patient were computed, exploring the feasibility of unsupervised methods in detecting clusters.

Utilizing the pairwise distance information, a multidimensional scaling (MDS) tool was employed to visualize

the data in three-dimensional space. Finally, a K-means algorithm was implemented using the MDS embeddings to uncover potential groupings or clusters within the data.

3. Results

Following preprocessing of ECG signals for each patient, the data was normalized to represent each heartbeat as a probability distribution. During initial analysis, variations in the starting time points for heartbeat segmentation among patients were noted. To address this, all heartbeats were adjusted so that the highest peak fell at the center of the distribution array.

For instance, Figure 1 illustrates a test file where all heartbeats are plotted in black, and the computed Wasserstein barycenter is highlighted in red. Utilizing both Euclidean and Wasserstein barycenters, we observed the ability to summarize the collective behavior of all heartbeats into a single distribution.

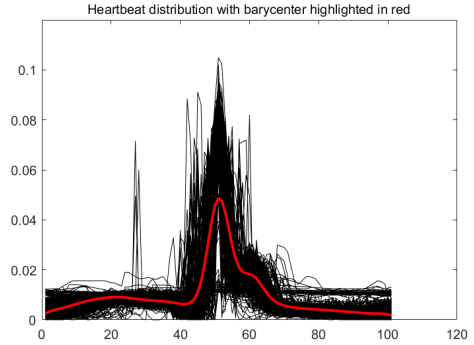


Figure 1. Heartbeat distribution of a test file with Wasserstein barycenter highlighted in red.

Various metrics were computed, including barycenters (Euclidean and Wasserstein) per patient and per recording, along with pairwise distances of heartbeats. These distances were depicted as a square metric D_{ij} , representing the dissimilarity between heartbeat distributions i and j . Subsequently, these distance matrices were employed for an MDS embedding into a three-dimensional space, as showcased in Figure 2. This demonstrated the geometric clustering of heartbeats into different groups (sinus or JET) using distance metrics.

To visualize the temporal dynamics of heartbeats, MDS embeddings were utilized for Kmeans clustering. Kmeans identifies distinct clusters in the data and assigns each heartbeat accordingly. As an unsupervised method, Kmeans does not rely on predefined labels, revealing inherent patterns among different heartbeat categories.

Figure 3 showcases individual patient plots, with the x-axis indicating heartbeat index and the y-axis representing probability values. The heartbeat were ordered chronologically to observe temporal changes. For each patient, Kmeans was computed with $k = 4$ to identify multiple clusters. Subsequently, a window size of 10 was employed to determine the percentage of heartbeats within each cluster. In

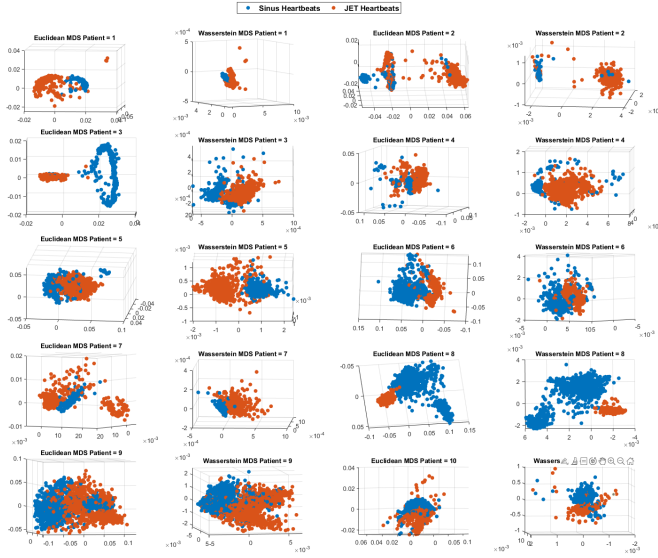


Figure 2. 3D MDS embedding of the data per patient. On each row, both Euclidean and Wasserstein MDS are shown side by side for 10 different patients. Heartbeats are labeled as sinus (blue) and JET (red) heartbeats. The results show that for some of the patients, there is a clear separation among heartbeats of different groups when using 3D MDS.

Figure 3, it's evident that while some patients exhibit all JET heartbeats grouped into a single cluster (as depicted in the bottom left plot), others display multiple clusters for both JET and sinus heartbeats. These results reveal intermediate stages or clusters that may exhibit characteristics from both groups, indicating nuances between pure sinus and JET categories.



Figure 3. KMeans analysis per patient with $k=4$. Each plot represents how the membership of the heartbeats changes over time. For some of the patients, a clear cluster representing the JET heartbeats was found, but for others multiple clusters were found for each of the categories (sinus or JET) which can be interpreted as new labels or intermediate stages.

In a different analysis using the patient data, heartbeats

were grouped without initially performing MDS embedding. Instead, Kmeans with $k = 2$ was employed using the original heartbeat distribution to discover behavioral changes as patients transitioned from sinus to JET heartbeats. Results indicated KMeans can identify two distinct clusters within the data. Notably, the distances between each heartbeat and the centroids of these clusters varied as patients transitioned from sinus to JET beats. This suggests a correspondence between the clusters identified by KMeans and the categories of sinus and JET heartbeats.

However, for other patients, the distance change between sinus and JET heartbeats was less pronounced, implying the potential existence of more than two distinct clusters within their data. This variation indicates the complexity and potential diversity in clustering patterns among different patients.

4. Discussion

The main goal of this report was to evaluate the effectiveness of geometric-based metrics in distinguishing between a healthy sinus heartbeat and a JET heartbeat. Initial findings indicate discernible differences between these categories; however, these distinctions vary among individual patients.

Clustering results from the MDS embedding reveal a geometric segregation in the data, for example, as seen in patient 3. Additionally, indications suggest the existence of more than two clusters, implying a potential transitional phase between sinus and JET heartbeats. Identifying what this transitional stage looks like could prove essential for early JET arrhythmia detection.

Notably, Wasserstein metrics, observed in patients 5, 6, 7, 8, 9, and 10, exhibited superior separation compared to Euclidean metrics when the data was reduced to three dimensions. However, expanding this analysis to higher dimensions is the subsequent focus of this project. This approach could reveal more interesting findings in cases be useful in cases where there is no clear clustering of data in lower dimensions.

The results also varied significantly per patient, which suggests that the geometric aspect of JET heartbeats may not be consistent universally. Hence, a personalized algorithmic framework is needed to accurately identify JET heartbeats on an individual basis. The next phase will involve analyzing differences in centroids among patients to uncover potential global data variations.

These visualizations uncovered possible data labeling errors. For example, in some of the patients, heartbeats labeled as sinus exhibited close proximity to JET heartbeats. However, further research is needed to rule out the possibility of these heartbeats belonging to unidentified third category.

A limitation of this research comes from the data segmentation process. Since geometric based methods are computed on the data, the alignment of the heartbeats is crucial to accurately describe their behavior. To mitigate this problem, the heartbeats were processed so that their highest

peak occurred at the midpoint; however, this may not be the case for all patients. In the next stage of this project will explore different technique to improve segmentation accuracy.

Acknowledgments

Matlab and Python script were used for the processing, analysis, and visualization of the data. The author declare no potential conflicts of interest. This work was supported by the assistance of Dr. Cesar Uribe from Rice University and Dr. Sebastian Acosta from Baylor College of Medicine as Principal Investigators.

References

- [1] S.S. Abeysekera. An efficient hilbert transform interpolation algorithm for peak position estimation. In *Proceedings of the 11th IEEE Signal Processing Workshop on Statistical Signal Processing (Cat. No.01TH8563)*, pages 417–420. IEEE, 2001.
- [2] Jérémie Bigot, Elsa Cazelles, and Nicolas Papadakis. Penalization of barycenters in the wasserstein space. *SIAM journal on mathematical analysis*, 51(3):2261–2285, 2019.
- [3] David C Gaze. Introductory chapter: Congenital heart disease. IntechOpen, 2018.
- [4] MD Haas, Nikolaus A. and MD Camphausen, Christoph K. Impact of early and standardized treatment with amiodarone on therapeutic success and outcome in pediatric patients with postoperative tachyarrhythmia. *The Journal of thoracic and cardiovascular surgery*, 136(5):1215–1222, 2008.
- [5] Michael C. Hout, Megan H. Papesh, and Stephen D. Goldinger. Multidimensional scaling. *Wiley interdisciplinary reviews. Cognitive science*, 4(1):93–103, 2013.
- [6] Nasser Kehtarnavaz. Chapter 7 - frequency domain processing. In Nasser Kehtarnavaz, editor, *Digital Signal Processing System Design (Second Edition)*, pages 175–196. Academic Press, Burlington, second edition edition, 2008.
- [7] Mariano Llamedo and Juan Pablo Martinez. Heartbeat classification using feature selection driven by database generalization criteria. *IEEE transactions on biomedical engineering*, 58(3):616–625, 2011.
- [8] Parul Madan, Vijay Singh, Devesh Pratap Singh, Manoj Diwakar, Bhaskar Pant, and Avadh Kishor. A hybrid deep learning approach for ecg-based arrhythmia classification. *Bioengineering (Basel)*, 9(4):152–, 2022.
- [9] JEFFREY P. MOAK, PATRICIO ARIAS, JONATHAN R. KALTMAN, YAO CHENG, ROBERT MCCARTER, SRIDHAR HANUMANTHATHIAH, GERARD R. MARTIN, and RICHARD A. JONAS. Postoperative junctional ectopic tachycardia: Risk factors for occurrence in the modern surgical era. *Pacing and clinical electrophysiology*, 36(9):1156–1168, 2013.
- [10] Victor M Panaretos and Yoav Zemel. Statistical aspects of wasserstein distances. *Annual review of statistics and its application*, 6(1):405–431, 2019.
- [11] Gabriel Peyré and Marco Cuturi. Computational optimal transport. *arXiv.org*, 2020.
- [12] Denise van der Linde, Elisabeth E M Konings, Maarten A Slager, Maarten Witsenburg, Willem A Helbing, Johanna J M Takkenberg, and Jolien W Roos-Hesselink. Birth prevalence of congenital heart disease worldwide: a systematic review and meta-analysis. *Journal of the American College of Cardiology*, 58(21):2241–2247, 2011.
- [13] Jamie L.S. Waugh, Raajen Patel, Yilong Ju, Ankit B. Patel, Craig G. Rusin, and Parag N. Jain. A novel automated junctional ectopic tachycardia detection tool for children with congenital heart disease. *Heart rhythm O2*, 3(3):302–310, 2022.